

1 **Enhancing grain size in durum wheat using RNAi to knock-down *GW2***

2 Francesco Sestili¹, Riccardo Pagliarello¹, Alessandra Zega², Rosaria Saletti², Anna Pucci¹, Ermelinda Botticella¹, Stefania
3 Masci¹, Silvio Tundo¹, Ilaria Moscetti¹, Salvatore Foti², Domenico Lafiandra¹

4

5 ¹Department of Agriculture and Forest Sciences, University of Tuscia, Via S. Camillo de Lellis, 01100 Viterbo, Italy

6 ²Department of Chemical Sciences, University of Catania, Viale A. Doria 6, 95125 Catania, Italy

7

8 Francesco Sestili: francescosestili@unitus.it ORCID: 0000-0002-9653-8002

9 Riccardo Pagliarello: riccardopagliarello@yahoo.com

10 Alessandra Zega: alessandra.zega@libero.it

11 Rosaria Saletti: rsaletti@unict.it

12 Anna Pucci: a.pucci@unitus.it

13 Ermelinda Botticella: e.botticella@unitus.it

14 Stefania Masci: masci@unitus.it ORCID: 0000-0003-2857-4498

15 Silvio Tundo: silvio.tundo@gmail.com

16 Ilaria Moscetti: ilariamoscetti@gmail.com

17 Salvatore Foti: sfoti@unict.it

18 Corresponding author: Domenico Lafiandra: lafiandr@unitus.it phone: +39 0761 357343 ORCID: 0000-0003-2805-
19 3932

20

21 This paper is dedicated to the memory of our colleague and friend Prof. Renato D'Ovidio.

22

23 **Abstract**

24 Raising crop yield is a priority task in the light of the continuing growth of the world's population and the inexorable
25 loss of arable land to urbanization. Here, the RNAi approach was taken to reduce the abundance of *GW2* transcript in
26 the durum wheat cultivar Svevo. The effect of the knock-down was to increase the grains' starch content by 10-40%,
27 their width by 4-13% and their surface area by 3-5%. Transcriptomic profiling, based on a quantitative real time PCR
28 platform, revealed that the transcript abundance of genes encoding both cytokinin dehydrogenase 1 and the large
29 subunit of ADP-glucose pyrophosphorylase was markedly increased in the transgenic lines, whereas that of the genes
30 encoding cytokinin dehydrogenase 2 and gibberellin 3-oxidase was reduced. A proteomic analysis of the non-storage
31 fraction extracted from mature grains detected that some seven proteins were differentially represented in the transgenic
32 compared to wild type grain: some of these were involved in, or at least potentially involved in cell wall development,
33 suggesting a role of *GW2* in the regulation of cell division in the wheat grain.

34

35 **Keywords:** durum wheat, yield, RNA interference, grain size, *GW2*

36 **Key message:** Knocking-down *GW2* enhances grain size by regulating genes encoding the synthesis of cytokinin,
37 gibberellin, starch and cell walls.

38 **Introduction**

39 Durum wheat (*T. turgidum ssp durum*) is an allotetraploid species used primarily for the preparation of pasta, couscous
40 and bulgur. The crop is produced mainly in southern Europe, North Africa and North America, but significant quantities
41 are also produced in the central Asia and India (Kadkol and Sissons 2016). Although the productivity of durum wheat is
42 below that of bread wheat, the demand for its grain has been rising from year to year.

43 Crop yield is both a genetically complex trait, and one which is strongly influenced by environmental factors. The grain
44 yield of wheat is conventionally expressed as the product of a number of sub-traits, namely the mean weight of each grain,
45 the number of grains set per spike and the number of fertile spikes per unit area (Sreenivasulu and Schnurbusch, 2012).

46 Although various genetic analyses have mapped a number of loci associated with wheat grain size in durum wheat, the
47 species' tetraploid nature tends to hinder attempts to isolate the genes underlying these effects (Bednarek et al. 2012;
48 Hong et al. 2014; Simmonds et al. 2016). The situation is rather different in the diploid species rice, where a number of
49 genes controlling grain size and shape have been mapped and/or isolated (Xing and Zhang, 2010; Zhang et al. 2013). A
50 prominent such gene is Grain Weight 2 (*OsGW2*) which encodes a RING-type protein exhibiting E3 ubiquitin ligase
51 activity and thought to be involved in the regulation of cell division (Song et al. 2007). In genotypes lacking a functional
52 copy of *GW2*, grain fill is accelerated, leading to an increase in grain weight and width, while in *GW2* over-expressors,
53 grain size is diminished (Song et al. 2007). The maize (a cryptic tetraploid) genome harbors two copies of *GW2*; sequence
54 variation in the promoter region of one of these has been significantly associated with variation in both the width and
55 weight of the kernels (Li et al. 2010). Meanwhile in the hexaploid bread wheat genome, *GW2* homologs have been mapped
56 to the short arm of the each of the homeologous group 6 chromosomes (Su et al. 2011). A negative relationship has been
57 established between the abundance of the A genome homeolog (*TaGW2-A1*) and grain weight (Su et al. 2011; Zhang et
58 al. 2013; Jaiswal et al. 2015; Simmonds et al. 2016), while sequence variants in *TaGW2-A1*'s promoter region have been
59 associated with diversity both with respect to the gene's transcript abundance and grain width (Su et al. 2011; Zhang et
60 al. 2013; Jaiswal et al. 2015). Simmonds et al. (2016) have reported an induced null mutant for *TaGW2-A1*; its associated
61 phenotype was a significant increase in the mean weight, width and length of the grain.

62 The RNA interference (RNAi) platform, in which synthetic RNA sequences are introduced into cells in order to
63 selectively and robustly induce the suppression of a specific target gene, has twice been used to study the effect of
64 knocking down all three bread wheat *TaGW2* homeologs, but the results obtained have been inconsistent: thus while
65 Bednarek et al. (2012) observed a reduction in grain size and cell number in the endosperm, Hong et al. (2014) reported
66 a significant increase in both grain width and weight. Here, a similar approach was taken, this time at the durum wheat
67 level. Care was taken in designing the transgene to include a grain-specific promoter, so that alterations in the expression
68 of the *TaGW2* homeologs in non-grain tissue was avoided.

69

70 **Materials and methods**

71 **Plant material and growing conditions**

72 Seedlings of wild type (WT) durum wheat cultivar (cv.) Svevo and three derived RNAi transgenics were vernalized by
73 holding at 4°C for four weeks, after which the plants were raised in a regime of 20-28°C during the lit period (16 h) and
74 16-24°C during the dark period (8 h); the light intensity was 300 $\mu\text{E m}^{-2}\text{s}^{-1}$.

75

76 **Isolation of GW2 sequences from durum wheat and their phylogeny**

77 *GW2-A1* and *-B1* sequences were isolated from the durum wheat genome database (<http://d-data.interomics.eu/>). A
78 phylogenetic analysis, based on their deduced polypeptide sequences, was carried out using the Neighbor Joining method,
79 as implemented in the MEGA v7 software package (www.megasoftware.net/), applying 1,000 bootstrapping replications
80 (Felsenstein 1985).

81

82 **The RNAi cassette and the biolistic transformation of immature embryos**

83 The segment of *TaGW2-B1* (GenBank accession KJ697755.1) lying between nucleotides 838 and 1,259 was PCR
84 amplified from a template of RNA extracted from cv. Svevo grains harvested at 21 days post anthesis. Extraction of the
85 necessary RNA and its conversion to ss cDNA followed protocols described by Sestili et al. (2015). The PCRs were based
86 on the primer pair XbaI/SalI/BamHI-GW2F and XbaI/XhoI/KpnI-GW2R (Table S1) in a 50 μL reaction containing 2 μL
87 cDNA, 25 μL GoTaq® Hot Start Color-less Master Mix (Promega, Madison, WI, USA) and 0.5 μM of each primer. The
88 resulting amplicon was introduced in both its sense and antisense direction into the plasmid pRDPT (Tosi et al. 2004)
89 using, respectively, the SalI/KpnI and XbaI/XhoI restriction sites. The result was a construct termed RDPT-GW2(RNAi)
90 (Fig. S1). The transgene was placed under the control of an endosperm-specific promoter (Sestili et al. 2010). About
91 3,000 immature cv. Svevo embryos were co-bombarded with a 3:1 molar ratio of pRDPT-GW2(RNAi) and pAHC20
92 (Christensen and Quail, 1996), as described by Sestili et al. (2010). The pAHC20 construct harbors *Bar*, the product of
93 which confers resistance to the herbicide bialaphos, thereby providing a selectable marker for recognizing transgenic
94 regenerants.

95

96 **PCR-based validation of putative transgenic plants**

97 Genomic DNA was extracted from young leaves of T_0 regenerants using a NucleoSpin® Plant II Mini Kit (Macherey
98 Nagel, Düren, Germany). The presence of the two transgenes was PCR-validated, using as primer pairs both pRDPT-
99 Fw/Rev and BarFw/Rev (Table S1). Each 20 μL reaction contained 10 μL Hot GoTaq® Green Master Mix (Promega,

100 Madison, WI, USA), 50 ng genomic DNA and 0.5 μ M of each primer, and was subjected to a 95°C/2 min denaturation,
101 followed by 35 cycles of 95°C/1 min, 60°C/1 min, 72°C/1 min, ending in a final extension step of 72°C/5 min. The
102 amplicons were electrophoretically resolved through 1.5% agarose gels and visualized by EtBr staining.

103

104 **RNA extraction and transcription profiling**

105 Total RNA was extracted from embryos formed in WT and RNAi transgenic grains harvested 21 days post anthesis, using
106 a Spectrum Plant Total RNA kit (Sigma-Aldrich, St. Louis, MO, USA). A 1 μ g aliquot of RNA represented the template
107 for the synthesis of ss cDNA, achieved using a QuantiTect Reverse Transcription Kit (Qiagen, Hilden, Germany).
108 Quantitative real time PCRs (qRT-PCRs) were performed using a CFX 96 Real-Time PCR Detection System device (Bio-
109 Rad, Hercules, CA, USA), following the procedure described by Camerlengo et al. (2017). Relative transcript abundances
110 were estimated using the $2^{-\Delta\Delta C_t}$ method (Livak and Schmittgen, 2001). The chosen reference sequence was β -actin. The
111 relevant primer pairs are listed in Table S1. Each genotype was represented by three biological replicates, each of which
112 in turn was associated with three technical replicates.

113

114 **Grain and spike phenotype**

115 The following traits were monitored from physiologically mature plants: the number of spikelets per spike (SS), the
116 weight of each spike (SW), the number of spikes per plant (SP), the surface area (GA), perimeter (GP), length (L) and
117 width (W) of each grain and the weight of 100 grains (HGW). The various grain traits were obtained from scanned images
118 of a sample of 100 grains of both WT and each RNAi line, obtained using a Perfection V750 PRO scanner (Epson Italia
119 S.p.A., Milano, Italy) in conjunction with SilverFast v.6.5.0r4e software (www.silverfast.com). The trait values were
120 derived using SmartGrain software (Tanabata et al. 2012) (www.kazusa.or.jp/phenotyping/smartgrain/index.html). The
121 starch content of single grains (TS) was obtained using a Total Starch Assay kit (AA/AMG) (Megazyme Pty Ltd.,
122 Wicklow, Ireland), following manufacturer's protocol. Each line was represented by three biological replicates.

123

124 **Statistical analysis**

125 Grain yield and grain size traits have been expressed in the form mean \pm standard error. Significant differences between
126 mean values were identified by applying a one-way analysis of variance, in conjunction with the post hoc Tukey HSD
127 test. Significant differences were confirmed using the Scheffé, Bonferroni and Holm multiple comparison tests. The
128 significance threshold was set at 0.05.

129

130 **Extraction from flour of the metabolic fraction**

131 Three replicate 200 mg samples of flour milled from the grain of either WT or transgenic line IM17-33aII were each
132 suspended in 2 mL 0.4 M NaCl, 0.067 M NaH₂PO₄ (pH 7.6). The suspensions were mixed for 15 min, centrifuged (12.000
133 rpm, 10 min, 4°C) and the supernatant was retained. The procedure was repeated two more times, and the three
134 supernatants were pooled and the final volume made up to XXX mL. The concentration of protein in each pooled sample
135 was determined using a Qubit™ Protein Assay kit, (ThermoFisher Scientific, Milan, Italy). An aliquot containing ~50
136 µg protein (typically around 20 µL) was lyophilized under vacuum, and dissolved in 20 mM ammonium bicarbonate (pH
137 8.3) to give a concentration of 1 µg protein per µL; 0.4 µg of chicken lysozyme was added to provide an internal standard.
138 Disulfide bridges were disrupted by the addition of 38.9 µg DTT dissolved in XX µL of the same buffer, followed by a 3
139 h incubation in the dark at 25°C. Alkylation was performed by the addition of iodoacetamide at the same molar ratio over
140 total thiol groups and the reaction was allowed to proceed for 1 h in the dark at 25°C. The reduced and alkylated proteins
141 were finally subjected to tryptic digestion by incubation with modified porcine trypsin in ammonium bicarbonate (pH
142 8.3) at an enzyme-substrate ratio of 1:50 at 37°C for 4 h. The digests were made up to 2 mL with 5% aqueous FA and
143 analyzed using a nano UHPLC/High Resolution nano ESI-MS/MS.

144

145 Liquid chromatography and tandem mass spectrometry

146 Mass spectrometry (MS) data were acquired using an Orbitrap Fusion Tribrid (Q-OT-qIT) mass spectrometer
147 (ThermoFisher Scientific, Bremen, Germany) equipped with a ThermoFisher Scientific Dionex UltiMate 3000 RSLC nano
148 system (Sunnyvale, CA, USA). A 1 µL aliquot of the digestion was loaded onto an Acclaim® Nano Trap C18 column
149 (100 µm i.d. × 2 cm, 5 µm particle size, 100 Å). After rinsing the trapping column with solvent A (aqueous 0.1% FA) for
150 3 min at a flow rate of 7 µL/min, peptides were eluted from the trapping column onto a PepMap® RSLC C18 EASY-
151 Spray, 75 µm × 50 cm, 2 µm, 100Å column and were separated by elution at a flow rate of 0.25 µL/min at 40°C, with a
152 linear gradient of solvent B in A from 5% to 65% over 82 min, followed by 65% to 95% over 5 min, at 95% for 5 min
153 and finally from 95% to 5% over 10 min. The eluted peptides were ionized by a nanospray (Easy-spray ion source,
154 Thermo Scientific) using a spray voltage of 1.7 kV and introduced into the mass spectrometer through a heated ion transfer
155 tube (275°C). Survey scans of peptide precursors in the *m/z* range 400–1600 were performed at a resolution of 120,000
156 (@ 200 *m/z*) with a AGC target for Orbitrap survey of 4.0 × 10⁵ and a maximum injection time of 50 ms. Tandem MS
157 was performed by isolation at 1.6 Th with the quadrupole, and high energy collisional dissociation (HCD) was performed
158 in the Ion Routing Multipole (IRM), using a normalized collision energy of 35 and rapid scan MS analysis in the ion trap.
159 Only precursors with a charge state of 2–4 and an intensity above the threshold of 5,000 were sampled for MS². The
160 dynamic exclusion duration was set to 60 s with a 10 ppm tolerance around the selected precursor and its isotopes.
161 Monoisotopic precursor selection was turned on. AGC target and maximum injection time (ms) for MS/MS spectra were

Commentato [1]: Meaning 100% unclear

Commentato [2]: Meaning?

Commentato [3]: Meaning?

Commentato [4]: What is solvent B?

162 10,000 and 100, respectively. The instrument was run in top speed mode with 3 s cycles, meaning the instrument
163 continuously performed the MS² events until the list of non-excluded precursors diminished to zero or 3 s, whichever
164 occurred soonest. MS/MS spectral quality was enhanced by enabling the parallelizable time option (i.e. by using all
165 parallelizable time during full scan detection for MS/MS precursor injection and detection). Each WT and transgenic line
166 extract was injected in triplicate, in order to assess the reproducibility of the MS data. This generated a total of 18 MS
167 data sets. MS calibration was performed using the Pierce® LTQ Velos ESI Positive Ion Calibration Solution (Thermo
168 Fisher Scientific). MS data acquisition was performed using the Xcalibur v. 3.0.63 software (Thermo Fisher Scientific).

169

170 **Database search**

171 The LC-MS/MS data were processed using PEAKS software v. 8.5 (Bioinformatics Solutions Inc., Waterloo, ON,
172 Canada). The data were searched against the 881,439 entry “Wheat” UniProt database (SwissProt and trEMBL, release
173 March 2018). Tryptic peptides with a maximum of three missed cleavage sites were subjected to an *in silico* search.
174 Cysteine carboxyamidomethylation was set as a fixed modification, whereas oxidation of methionine, and transformation
175 of N-terminal glutamine and N-terminal glutamic acid residues in the form of pyroglutamic acid were classed as variable
176 modifications. The precursor mass tolerance threshold was 10 ppm and the maximum fragment mass error was set to 0.6
177 Da. Peptide spectral matches (PSM) were validated using Target Decoy PSM Validator node based on q-values at a 0.1%

178 **FDR**. A protein was considered as identified if a minimum of two peptides matched and if its coverage was $\geq 5\%$ in at
179 least two biological replicates and in two technical replicates of either the WT or the transgenic line. Proteins containing
180 the same peptides which could not be differentiated based on MS/MS analysis alone were grouped to satisfy the principles
181 of parsimony. Label-free quantification data were obtained using PEAKS Q software, which detected the reference sample
182 and automatically aligned the sample runs. Proteins present in distinctly different concentrations between the two
183 genotypes were identified by a statistical analysis tool (protein fold change ≥ 2 , protein significance ≥ 20 , and unique
184 peptides ≥ 1). The data have been displayed in a heatmap format for ready visualization.

185

186 **Results**

187 **The GW2 proteins formed by WT cv. Svevo**

188 The *TaGW2-A1* and *-B1* cDNA sequences (GenBank accessions AFU88754 and AFU88755, respectively) were used to
189 identify the corresponding genomic regions in the cv. Svevo genome as mapping to the short arms of chromosomes 6A
190 and 6B. The sequences of the two homeologs were closely related to one another both at the nucleotide (98.3% identity)
191 and at the polypeptide (96.9% identity) levels (Fig. S2 and S3). The coding sequence length of both genes was 1,275 nt;
192 it was interrupted in both by seven introns, producing a predicted 424 residue product of molecular weight ~47 kDa (Fig.

Commentato [5]: Meaning?

Commentato [6]: Meaning?

193 S3). The 21 nucleotide polymorphisms which distinguished the two sequences (Fig. S2) were predicted to generate 13
194 residue differences. Both products' N-termini harbored two highly conserved sequences, namely the NES motif
195 LRKLILE and the 43 residue RING domain identified by Song et al. (2007) (Fig. S3). The former is shared with GW
196 homologs encoded by a number of grass species genomes, including those of barley, rice, maize, sorghum, *Brachypodium*
197 *distachyon* and foxtail millet; the latter is present in each of barley, maize, sorghum, *B. distachyon* and foxtail millet, but
198 in rice, the identity of the position 96 residue differs (Fig. S4). A phylogenetic analysis of the GW2 polypeptide sequences
199 revealed that the wheat GW2 proteins were most closely related to that of barley (Fig. 1).

200

201 **The production of GW2-RNAi transgenics**

202 A total of 850 immature cv. Svevo embryos was bombarded with pRDPT-GW2(RNAi) and pAHC20, from which 25
203 putative transgenic plants were regenerated. A PCR-based assay confirmed the presence of both pRDPT-GW2(RNAi)
204 and pAHC20 of 14 of these plants, while eight harbored only pAHC20 and three lacked both transgenes. After self-
205 pollination to the T₂ generation, it was possible to identify transgene homozygotes using the same PCR assays (Table S2).
206 The three independent homozygous transgenic lines IM17-15a, -33aII and -81 were carried forward for the subsequent
207 experiments.

208

209 **The abundance of GW2 transcript in the transgenic lines**

210 The abundance of GW2 transcript in the three GW2-RNAi lines was estimated by a qRT-PCR assay based on three set
211 sets of primer pairs, two of which were homeolog-specific and one of which recognized both homeologs. Immature grains,
212 harvested 21 days post anthesis, were sampled from three independent plants per each line. Transcription from both
213 homeologs was equally affected. The abundance of GW2 transcript was reduced by >75% in all three GW2-RNAi lines,
214 with some variation seen in the extent of the knock-down between the lines: the reduction was 76% in IM17-81, 81% in
215 IM17-15a and 87% in IM17-33aII (Fig. 2).

216

217 **The effect of GW2 down-regulation on grain phenotype**

218 The effect of GW2 down-regulation on the set of grain and spike traits (HGW, SW, SP, SS, TS, GA, GP, GL and GW)
219 was assessed by comparing the performance of the three transgenic lines with that of WT plants. Significant differences
220 were observed for several of the traits. In IM17-33aII, HGW was raised by 18%, SW by 20%, GA by 13%, GP by +7%,
221 GL by 7% and GW by 5% (Tables 1 and 2; Fig. 3). GW and GA were increased by, respectively, 4-13% and 3-5% across
222 the three transgenic lines., whereas HGW and GL were enhanced only in IM17-33aII. As anticipated (since the transgene
223 promoter was endosperm-specific), neither SP nor SS was altered. With respect to SW, the increase experienced by IM17-

224 33aII was accompanied by a fall of ~25% in each of the other two transgenic lines. TS measured from flour samples was
225 not significantly affected by the presence of the transgene, but when assessed on a single grain basis, its level proved to
226 be significantly higher in both IM17-15a (by 40%) and IM17-33aII (by 31%).

227

228 **Differentially expressed proteins (DEPs) in the metabolic fraction of the mature grain proteome**

229 An exploration of the proteomic effect of *GW2* knock-down was explored using the contrast between WT and line IM17-
230 33a. The RP-nUHPLC/nESI-MS/MS analyses and subsequent database search against the “*Wheat*” UniProt database
231 identified a set of 2,613 proteins in Svevo and 2,672 in the transgenic line IM17-33aII (Table S3), among which was a
232 considerable number of uncharacterized proteins. Of these, based on a threshold of an at least two fold difference in
233 abundance, eleven were classed as DEPs (Fig. 4). One of these was present at below the level of detection in IM17-33a
234 grain, while the other ten were more abundant in the transgenic grain (Fig. 4; Table S4). The former carried a sequence
235 of seven residues found in two different proteins, one of which is uncharacterized, while the other has been identified as
236 a xylanase inhibitor (Figs S5a, S6a). Among the ten proteins which were more abundant in the transgenic grain, the
237 function of five was inferred based on a sequence coverage ranging from 20-75% (Tables S4, S5). Two of these five were
238 very highly similar to one another (differing by just one residue, see Fig. S6b): one was classified as a CM16 α -
239 amylase/trypsin inhibitor and the other as a CM16 major allergen. A group of seven peptides was shared by four of the
240 proteins, two of which are uncharacterized, whereas the other two resembled the 60S ribosomal protein L23a either
241 present in the diploid wheat *T. urartu* (Fig. S6c,d) or in the wheat D genome donor species *Aegilops tauschii* (Fig. S6e).
242 A BLAST search (blast.ncbi.nlm.nih.gov/Blast.cgi) detected eight peptides in one of the three uncharacterized proteins,
243 and 18 in a second one which matched the sequence of a trypsin/ α -amylase inhibitor harbored by *T. urartu* (Fig. S6f,g).
244 The third protein featured a sequence similarity of 99.3% with a *B. distachyon* farinin protein (Fig. S6h).

245

246 **The transcriptional consequences of knocking down GW2**

247 The transcriptional behavior in the transgenic lines of four genes documented as being responsive to the knocking down
248 of *GW2-A1* in bread wheat (Geng et al. 2017; Li et al. 2017) was examined via qRT-PCR: the genes included two encoding
249 a cytokinin dehydrogenase (*CKX1*, *CKX2*), one a gibberellin oxidase (*GA3-ox*) and one a large subunit of ADP-glucose
250 pyrophosphorylase (*AGPL*). Both *CKX1* and *AGPL* proved to be up-regulated in all three transgenic lines, the former by
251 2.2-3.2 fold and the latter by 1.7-2.3 fold (Fig. 4a). *CKX2* and *GA3-ox* behaved very differently: both were down-regulated
252 in IM17-33a and IM17-81, but the abundance of their transcript was unaltered in IM17-15a. The qRT-PCR platform was
253 further used to explore the transcription in immature grain samples of some of the genes responsible for the DEPs. The

Commentato [7]: What follows is very muddled.

You say there were 10 proteins up-regulated in the transgenic grain, and that five were “specifically identified with a sequence coverage ranging from 20 to 75%”. Two of these 5 were similar to CM16 α -amylase/trypsin inhibitor and the other as a CM16 major allergen. Two were similar to 60S ribosomal protein L23a. What was the 5th one?

Then you say there were “three uncharacterized up-regulated proteins”, but I was expecting to see 5 of these (10 minus 5).

This was impossible to edit properly – you need to explain this more clearly to me. For the moment, all I have done is to correct the language, but you can’t leave it like this.

254 outcome of this analysis was consistent with the proteomic analysis with just one exception: *XIP-III* was down-regulated
255 in IM17-33a, whereas *CM3*, *CM16*, *EG11* and *nsLTP* were all up-regulated, by, respectively 2.8, 2.1, 4.5 and 1.8 fold
256 (Fig. 4b); the exception was a gene encoding farinin, which was not differentially transcribed in the immature grain.

257

258 Discussion

259 Grain weight is a key component of the economic yield of cereal crops. The impact of intensive selection for this trait has
260 been illustrated recently by a demonstration of the extent of the decline in sequence polymorphism remaining at *GW2* in
261 wheat since domestication (Qin et al. 2017). In cv. Svevo, the two *GW2* homeologs share a very high degree of homology,
262 both at the nucleotide and the polypeptide levels. The function of *GW2* is now well established in rice to be a negative
263 regulator of cell division, since loss-of-function mutants form larger grains weight as a result of their higher grain filling
264 rate (Song et al. 2007). In both bread and durum wheat, negative associations have been established between the
265 abundance of *GW2-A1* transcript and grain weight (Su et al. 2011; Yang et al. 2012; Zhang et al. 2013; Hong et al. 2014;
266 Jaiswal et al. 2015; Simmonds et al. 2016). Recently, a novel *GW2-A1* allele, lacking a 114 nt segment of the promoter
267 sequence, has been shown to result in a reduction in the gene's transcription (Zhai et al.2018); the same allele is present
268 in the Chinese bread wheat cultivar Lankaodali (unpublished data), which produces particularly long grains. According
269 to Hong et al. (2014), however, the abundance of both *TaGW2-B1* and *-D1* transcript appears to be positively associated
270 with grain width. An analysis of gene-editing derived knock-out mutants involving either one, two or all three bread wheat
271 *GW2* homeologs did not support the notion that the products of either the B or the D genome homeologs counteract the
272 action of *GW2-A1* (Zhang et al. 2018); rather, the phenotype of these mutants demonstrates that both products likely
273 participate in the negative regulation of grain width, modulating cell number and length in the grain outer pericarp.
274 Attempts to down-regulate the bread wheat *GW2* homeologs using RNAi technology, meanwhile, have given rise to
275 conflicting results. While Bednarek et al. (2012) reported the effect to be a major drastic reduction in grain size, Hong et
276 al. (2014) found the opposite to be the case. The discrepancy may be artefactual, since the use of the full length of the
277 *GW2* sequence for the purpose of RNAi could have generated unexpected off-target effects; alternatively the results may
278 reflect a background effect, since the two studies did not use the same bread wheat cultivar.

279 Here, the RNAi approach was used to simultaneously knock-down both durum wheat *GW2* homeologs. Following the
280 suggestion made by Hong et al. (2014), the RNAi cassette incorporated only part of the target sequence, and as an
281 additional measure, the transgene was placed under the control of an endosperm-specific promoter to ensure that it was
282 expressed only in the intended time and place. The resulting transgenics exhibited a major decrease in the abundance of
283 *GW2* transcript (by 76-87%), a level of effectiveness which was higher than that achieved in bread wheat by both Hong
284 et al. (2014) and Bednarek et al. (2012). The phenotypic effect of the knock-down was marked: although there was some

285 variability between the independent transgenics for certain of the traits, all three lines produced grain which showed a
286 pronounced increase in weight, consistent with the outcome of silencing *GW2* homeologs at the hexaploid level (Hong et
287 al. 2014; Zhang et al. 2018). In contrast to the experience of Zhang et al. (2018), there was no evidence of any grain
288 shriveling, perhaps because, unlike the situation where the genes had been completely disrupted, here there still remained
289 a low level of *GW2* transcript and hence, presumably also some *GW2* function.

290 An analysis carried out on the metabolic fraction of the mature grain proteome established that the abundance of seven
291 proteins varied significantly in the grain formed by WT and RNAi-*GW2* transgenic line IM17-33aII plants. A much larger
292 number of such proteins has been identified from a comparison between the immature grain proteome of the model bread
293 wheat cultivar Chinese Spring and that of a *GW2-A1* knock-out (Du et al. 2016). The likely most probable reason for such
294 a different outcome is that, here the analysis was performed on mature grains. Of the seven DEPs, at least three (EG11,
295 nsLTP2 and XIP-III) have some association with cell wall synthesis. Endo-1,4- β -D-glucanases are required for cell
296 expansion, since they act to cleave the β -1,4-glycosidic bonds present in cellulose and xyloglucan (Lopez-Casado et al.
297 2008; Glass et al. 2015). The nsLTPs are small proteins which mediate phospholipid transfer, participate in plant defense
298 against pests and act to enhance cell wall extension (Wang et al. 2012). According to Nieuwland et al. (2005), nsLTPs
299 are associated with hydrophobic wall compounds, causing non-hydrolytic disruption of the cell wall and subsequently
300 facilitating wall extension. XIP xylanase inhibitors act to slow the spread of fungal pathogens (Domez et al. 2010); in
301 durum wheat, to date only XIP-II has been characterized (Elliott et al. 2009), leaving the physiological function of XIP-
302 III as yet unknown. It has been suggested that xylanase activity is required for remodeling cell wall during the growth
303 and development of the cereal grain, so the possibility does exist that XIP inhibitors are used in a regulatory capacity
304 during this process (Gebruers et al. 2002). In the grain formed by line IM17-33aII plants, both EG11 and nsLTP2 were
305 more abundant than in WT grain, while XIP-III was not detectable in the former. The implication is that the knocking-
306 down of *GW2* in cv. Svevo reduced the rigidity of the cell walls, making it easier for the cells to expand. Among the other
307 DEPs present in higher abundance in the knock-down line's grain were proteins thought to act as α -amylase/trypsin
308 inhibitors; their potential involvement in the process of cell wall development has not been reported to date.

309 As well as affecting the grain proteome, the knock-down of *GW2* also had a transcriptomic footprint, particularly
310 involving genes encoding starch and phytohormone synthesis. In the transgenic lines, the gene encoding the large subunit
311 of AGPase, an enzyme which catalyzes the conversion of glucose-1-phosphate to pyrophosphate plus ADP-glucose (Jeon
312 et al. 2010), was strongly up-regulated. Consistent with an enhancement to AGPase activity, the starch content of the
313 transgenic grain was higher than that of the WT grain. A similar up-regulation of genes encoding AGPase occurs in bread
314 wheat lines silenced for *GW2-A1* (Geng et al. 2017). The cytokinins (CKs) and gibberellins (GAs) act as regulators for a
315 wide range of processes, from cell growth to seed development (Huttly and Phillips, 1995; Locascio et al. 2015; Zürcher

316 and Müller, 2016). In the grain, CKs are particularly prominent during periods of rapid cell division, but lose their
317 importance as maturity approaches, when cell expansion takes over from cell division (Locascio et al. 2015). In contrast,
318 GAs tend to accumulate both during the differentiation of the embryo and late during the grains' maturation phase
319 (Locascio et al. 2015). In the GW2 knock-down lines' grains, the abundance of *CKX1* transcript (a gene which encodes a
320 CK degrading enzyme) was higher than in the WT grain, while that of *CKX2* was lower. According to Geng et al. (2017),
321 the absence of a functional GW2-A1 results in a significant reduction in the abundance of at least three *CKX* genes (*CKX1*,
322 *CKX2* and *CKX6*), an observation taken to imply a heightened accumulation of CK; the conclusion was that GW2-A1 in
323 some way controls the expression of *CKX* genes. Once again, the most likely explanation for the lack of agreement with
324 the present observations lies in the different physiological stages chosen to sample the transcriptomes, although it is also
325 possible that the consequences of a complete abolition of *GW2* transcription differ from those caused by its less than
326 complete abolition. There was little evidence for any effect of *GW2* knock-down on the transcription of *GA3-ox* in either
327 IM17-15a or IM17-33aII grain, whereas it did have a marginal suppressive effect in IM17-81 grain. A rather different
328 scenario has been reported by Li et al. (2017), who observed a significant increase in the abundance of *GA3-ox* transcript
329 in grains harvested 20 days post anthesis from a bread wheat line silenced for *GW2-A1*. The gene's transcription however
330 fluctuated during grain development, being greatly down-regulated in very young grains (12 DPA), but up-regulated in
331 grains sampled at 15 DPA.

332

333 Here, the intention was to characterize the effect of knocking-down both of the *GW2* homeologs present in durum wheat.
334 A range of phenotypic, molecular, proteomic and biochemical data were used to confirm that the product of *GW2* acts as
335 negative regulator of grain yield in durum wheat grain. The finding offers the potential to exploit either natural or induced
336 mutants of *GW2* to raise the grain yield potential of a leading cereal crop species.

337

338 **Author contribution statement**

339 FS prepared the RNAi construct, performed the phylogenetic analysis, coordinated the experiments, analyzed the data
340 and drafted the manuscript in conjunction with DL. IM, ST and SM were responsible for the plant transformation. EB
341 identified homozygous transgenic lines. AP performed qRT-PCR analysis on *GW2* genes. RP collected the phenotypic
342 data and performed the qRT-PCR analysis of other genes. AZ, RS and SF performed the proteomic experiments and
343 interpreted the resulting data. DL conceived the research. All of the authors have read and approved the final manuscript.

344

345 **Acknowledgement**

346 The authors gratefully acknowledge the pre-publication access to the durum wheat genome sequence data given by Luigi
347 Cattivelli and the International Durum Wheat Genome Sequencing Consortium. The research was financially supported
348 by Italian Ministry of Education, University and Research (MIUR): project PRIN 2010Z77XAX_001 “Identification and
349 characterization of yield- and sustainability-related genes in durum wheat” and in the frame of the MIUR initiative
350 “Departments of excellence”, Law 232/2016.

351

352 **Compliance with ethical standards**

353 **Conflict of interest** The authors declare that they have no conflict of interest.

354

355

356

357 **References**

358 Bednarek J, Boulafloous A, Girousse C, Ravel C, Tassy C, Barret P, Bouzidi MF, Mouzeyar S (2012) Down-regulation of
359 the *TaGW2* gene by RNA interference results in decreased grain size and weight in wheat. *J Exp Bot* 63:5945–5955.

360 <https://doi.org/10.1093/jxb/ers249>

361 Christensen AH, Quail PF (1996) Ubiquitin promoter-based vectors for high level expression of selectable and/or
362 screenable marker genes in monocotyledonous plants. *Trans Res* 5:213-218.

363 Dornez E, Croes E, Gebruers K, De Coninck B, Cammue BP, Delcour JA, Courtin CM (2010) Accumulated evidence
364 substantiates a role for three classes of wheat xylanase inhibitors in plant defense. *Critic Rev Plant Sci* 29:244-264.

365 <https://doi.org/10.1080/07352689.2010.487780>

366 Du D, Gao X, Geng J, Li Q, Li L, Lv Q, Li X (2016) Identification of key proteins and networks related to grain
367 development in wheat (*Triticum aestivum* L.) by comparative transcription and proteomic analysis of allelic variants in

368 *TaGW2-6A*. *Front Plant Sci* 7, 922. <https://doi.org/10.3389/fpls.2016.00922>

369 Elliott G, Durand A, Hughes RK, D’Ovidio R, Juge N (2009) Isolation and characterisation of a xylanase inhibitor *Xip-*
370 *II* gene from durum wheat. *J Cereal Sci* 50:324-331. <https://doi.org/10.1016/j.jcs.2009.06.013>

371 Feldman M, Liu B, Segal G, Abbo S, Levy AA, Vega JM (1997) Rapid elimination of low-copy DNA sequences in
372 polyploid wheat: a possible mechanism for differentiation of homeologous chromosomes. *Genetics* 147:1381–1387.

373 Gebruers K, Courtin CM, Goesaert H, Campenhout SV, Delcour JA (2002) Endoxylanase inhibition activity in different
374 European wheat cultivars and milling fractions. *Cereal Chem* 79:613-616.

375 <https://doi.org/10.1094/CCHEM.2002.79.5.613>

376 Gu YQ, Coleman-Derr D, Kong X, Anderson OD (2004) Rapid genome evolution revealed by comparative sequence
377 analysis of orthologous regions from four *Triticeae* genomes. *Plant Physiol* 135:459-470.
378 <https://doi.org/10.1104/pp.103.038083>

379 Hong Y, Chen L, Du L-p, Su Z, Wang J, Ye X, Qi L, Zhang Z (2014) Transcript suppression of TaGW2 increased grain
380 width and weight in bread wheat. *Funct Integ Gen* 14: 341-349. Doi: 10.1007%2Fs10142-014-0380-5

381 Huttly AK, Phillips AL (1995) Gibberellin-regulated plant genes. *Physiol Plant* 95:310-317.

382 Jaiswal V, Gahlaut V, Mathur S, Agarwal P, Khandelwal MK, Khurana JP, Tyagi AK, Balyan HS, Gupta PK (2015)
383 Identification of novel SNP in promoter sequence of *TaGW2-6A* associated with grain weight and other agronomic traits
384 in wheat (*Triticum aestivum* L.). *PLoS ONE* 10:e0129400. <https://doi.org/10.1371/journal.pone.0129400>

385 Jaiswal V, Gahlaut V, Meher PK, Mir RR, Jaiswal JP, Rao AR, Balyan HS, Gupta PK (2016) Genome wide single locus
386 single trait, multi-locus and multi-trait association mapping for some important agronomic traits in common wheat (*T.*
387 *aestivum* L.). *PLoS ONE* 11:e0159343. <https://doi.org/10.1371/journal.pone.0159343>

388 Jeon JS, Ryoo N, Hahn TR, Walia H, Nakamura Y (2010) Starch biosynthesis in cereal endosperm. *Plant Physiol Biochem*
389 48:383-392. <https://doi.org/10.1016/j.plaphy.2010.03.006>

390 Kadkol G., Sissons M. 2016. Durum wheat: overview. In: Wrigley C, Corke H, Seetharaman K, Faubion J (eds)
391 *Encyclopedia of Food Grains*, 2nd edition, Academic Press Inc, San Diego, pp. 117-124.

392 Li Q, Li L, Liu Y, Lv Q, Zhang H, Zhu J, Li X (2017) Influence of TaGW2-6A on seed development in wheat by
393 negatively regulating gibberellin synthesis. *Plant Sci* 263:226-235. <https://doi.org/10.1016/j.plantsci.2017.07.019>

394 Li Q, Li L, Yang X, Warburton M, Bai G, Dai J, Li J, Yan J (2010) Relationship, evolutionary fate and function of two
395 maize co-orthologs of rice GW2 associated with kernel size and weight. *BMC Plant Biol* 10:143.
396 <https://doi.org/10.1186/1471-2229-10-143>

397 Nadolska-Orczyk A, Rajchel IK, Orczyk W, Gasparis S (2017) Major genes determining yield-related traits in wheat and
398 barley. *Theor Appl Genet* 130:1081-1098. Doi: 10.1007/s00122-017-2880-x

399 Nieuwland J, Feron R, Huisman BA, Fasolino A, Hilbers CW, Derksen J, Mariani C (2005) Lipid transfer proteins
400 enhance cell wall extension in tobacco. *Plant Cell* 17:2009-2019. <https://doi.org/10.1105/tpc.105.032094>

401 Qin L, Zhao J, Li T, Hou J, Zhang X, Hao C (2017) *TaGW2*, a Good Reflection of Wheat Polyploidization and Evolution.
402 *Front Plant Sci* 8:318. <https://doi.org/10.3389/fpls.2017.00318>

403 Sestili F, Janni M, Doherty A, Botticella E, D'Ovidio R, Masci S, Jones H, Lafiandra D (2010) Increasing the amylose
404 content of durum wheat through silencing of the *SBEIIa* genes. *BMC Plant Biol* 10: 144. <https://doi.org/10.1186/1471->
405 2229-10-144

406 Sestili F, Palombieri S, Botticella E, Mantovani P, Bovina R, Lafiandra D (2015) TILLING mutants of durum wheat
407 result in a high amylose phenotype and provide information on alternative splicing mechanisms. *Plant Sci* 233:127-133.
408 <https://doi.org/10.1016/j.plantsci.2015.01.009>

409 Sestili F, Sparla F, Botticella E, Janni M, D'Ovidio R, Falini G, Marri L, Cuesta-Seijo JA, Moscatello S, Battistelli A,
410 Trost P, Lafiandra D (2016) The down-regulation of the genes encoding Isoamylase 1 alters the starch composition of the
411 durum wheat grain. *Plant Sci* 252:230-238. <https://doi.org/10.1016/j.plantsci.2016.08.001>

412 Simmonds J, Scott P, Brinton J, Mestre TC, Bush M, Del Blanco A, Dubcovsky J, Uauy C (2016) A splice acceptor site
413 mutation in *TaGW2-A1* increases thousand grain weight in tetraploid and hexaploid wheat through wider and longer
414 grains. *Theor Appl Genet* 129:1099-1112. Doi: 10.1007/s00122-016-2686-2

415 Song X-J, Huang W, Shi M, Zhu M-Z, Lin H-X (2007) A QTL for rice grain width and weight encodes a previously
416 unknown RING-type E3 ubiquitin ligase. *Nat Genet* 39:623-630. <https://doi.org/10.1038/ng2014>

417 Sreenivasulu N, Schnurbusch T (2012) A genetic playground for enhancing grain number in cereals. *Trends Plant Sci*
418 17:91-101. <https://doi.org/10.1016/j.tplants.2011.11.003>

419 Su Z, Hao C, Wang L, Dong Y, Zhang X (2011) Identification and development of a functional marker of *TaGW2*
420 associated with grain weight in bread wheat (*Triticum aestivum* L.). *Theor Appl Genet* 122:211-223. Doi:
421 10.1007/s00122-010-1437-z

422 Tosi P, D'Ovidio R, Napier JA, Bekes F, Shewry PR (2004) Expression of epitope-tagged LMW glutenin subunits in the
423 starchy endosperm of transgenic wheat and their incorporation into glutenin polymers. *Theor. Appl. Genet.*108: 468-476.
424 <https://doi.org/10.1007/s00122-003-1459-x>

425 Wang NJ, Lee CC, Cheng CS, Lo WC, Yang YF, Chen MN, Lyu PC (2012) Construction and analysis of a plant non-
426 specific lipid transfer protein database (nsLTPDB). *BMC Genomics* 13:S9. <https://doi.org/10.1186/1471-2164-13-S1-S9>

427 Xing Y, Zhang Q (2010) Genetic and molecular bases of rice yield. *Annu Rev Plant Biol* 61:421-442.
428 <https://doi.org/10.1146/annurev-arplant-042809-112209>

429 Yang Z, Bai Z, Li X, Wang P, Wu Q, Yang L, Li L, Li X (2012) SNP identification and allelic-specific PCR markers
430 development for *TaGW2*, a gene linked to wheat kernel weight. *Theor Appl Genet* 125:1057-1068. Doi: 10.1007/s00122-
431 012-1895-6

432 Zhai H, Feng Z, Du X, Song Y, Liu X, Qi Z, Song L, Li J, Li L, Peng H, Hu Z, Yao Y, Xin M, Xiao S, Sun Q, Ni Z
433 (2018). A novel allele of *TaGW2-A1* is located in a finely mapped QTL that increases grain weight but decreases grain
434 number in wheat (*Triticum aestivum* L.). *Theor Appl Genet* 131:539-553. Doi: 10.1007/s00122-017-3017-y

435 Zhang X, Chen J, Shi C, Chen J, Zheng F, Tian J (2013) Function of *TaGW2-6A* and its effect on grain weight in wheat
436 (*Triticum aestivum* L.). *Euphytica* 192:347-357. <https://doi.org/10.1007/s10681-012-0858-y>

437 Zhang Y, Li D, Zhang D, Zhao X, Cao X, Dong L, Liu J, Chen K, Zhang H, Gao C, Wang D (2018) Analysis of the
438 functions of *TaGW2* homeologs in wheat grain weight and protein content traits. *Plant J* 94:857-866.
439 <https://doi.org/10.1111/tpj.13903>

440 Zürcher E, Müller B (2016) Cytokinin synthesis, signaling, and function-advances and new insights. *Int Rev Cell Mol*
441 *Biol* 324:1-38. <https://doi.org/10.1016/bs.ircmb.2016.01.001>

442
443

444 **Figure captions**

445 **Fig. 1** Phylogenetic analysis of the GW2 protein family. Bootstrap values relating to each node are shown. Ta: *T. aestivum*
446 (GenBank accessions AFU88754, AIT11539, AFU88755); SV: durum wheat cv. Svevo (isolated here); Tu: *T. urartu*;
447 Aet: *Ae. tauschii* (GenBank accession XP_020175675); Hv: barley (GenBank accession ABY51682); Bd: *B. distachyon*
448 (GenBank accession XP_003571977); Os: rice (GenBank accessions EF447275, AB031101, NP_001046414); Si: foxtail
449 millet (GenBank accession XP_004951330); Zm: maize (GenBank accessions AFW65938, AFW71120); Sb: sorghum
450 (GenBank accession XP_002453598)

451
452

453 **Fig. 2** The abundance of GW2 transcript in grain harvested 21 days post anthesis, as measured by qRT-PCR. Data
454 expressed in the form of fold differences between the abundance in the grain set by WT and each of the three independent
455 GW2-RNAi lines IM17-15a, IM17-33a and IM17-81 plants. Three sets of primer pairs were deployed, two of which each
456 targeted one homeolog, while the third recognized both. Data shown in the form mean \pm standard error (SE) ($n=3$). *:
457 means differ from one another significantly ($P \leq 0.05$)

458
459

460 **Fig. 3** Variation with respect to grain length and width between the GW2 knock-down line IM17-33aII and WT cv. Svevo
461

462 **Fig. 4** Proteins differentially abundant in the grain of WT cv. Svevo and that of transgenic line IM17-33aII. 1) Xylanase
463 inhibitor XIP-III OS=*Triticum aestivum* (GenBank accession Q4W6G2), 2) Globulin OS=*Triticum urartu* (GenBank
464 accession H9XH65), 3) 12S seed storage globulin 1 OS=*Triticum urartu* (GenBank accession M7ZK46), 4) Farinin
465 protein OS=*Brachypodium distachyon* (GenBank accession W8QN15), 5) Type 2 non specific lipid transfer protein
466 OS=*Triticum aestivum* (GenBank accession Q2PCC3), 6) Putative non-specific lipid-transfer protein OS=*Aegilops*
467 *tauschii* (GenBank accession M8BVH7), 7) Endoglucanase OS=*Triticum aestivum* (GenBank accession A0A1D6ADY9),

468 8) 60S ribosomal protein L23a OS=*Triticum urartu* (GenBank accession ???), 9) Trypsin/alpha-amylase inhibitor
469 CMX1/CMX3 OS=*Triticum urartu* (GenBank accession M8A1S2), 10) Trypsin/alpha-amylase inhibitor
470 CMX1/CMX3 OS=*Triticum urartu* (GenBank accession M8A1S2), 11) Alpha-amylase/trypsin inhibitor CM16
471 OS=*Triticum aestivum* (GenBank accession P16159). A 0.4 µg aliquot of chicken lysozyme was added to each 50 µg
472 sample as an internal standard. Three replicates of each of WT and the transgenic line were analyzed, with each replicate
473 represented by three technical replicates

474

475

476 **Fig. 5** Transcriptional behavior of (a) *CKX1*, *CKX2*, *GA3-ox* and *AGPL*, genes known to be responsive to *GW2* knock-
477 down, and (b) of genes encoding the DEPs. The template represented cDNA prepared from grains harvested 21 days post
478 anthesis. Data expressed in as fold differences between the abundance in WT and in IM17-33aII grain. *: means differ
479 significantly at $P \leq 0.05$

480

481 **Tables**

482 **Table 1** Variation between the RNAi transgenic line and WT plants with respect to the expression of the weight of 100
 483 grains (HGW), the weight of each spike (SW), total grain starch content (TS), the number of spikes per plant (SP) and
 484 the number of spikelets per spike (SS). Values followed by different letters differ significantly ($P \leq 0.01$) from one another.
 485 To facilitate comparisons, all values are also reported (in parentheses) in the form of a percentage of the corresponding
 486 WT value

Lines	HGW (g)	SW (g)	TS (mg/seed)	No. of spike per plant	No. of spikelets per spike
Svevo	5.42±0.12a (100)	2.58±0.15a (100)	37.85±1.51a (100)	5.72±0.38	12.53±0.43
IM17-15a	5.50±0.11a (101)	1.90±0.12b (74)	53.18±2.91b (140)	7.44±0.69	11.78±0.32
IM17-33aII	6.38±0.14b (118)	3.09±0.12c (120)	49.57±2.50bc (131)	6.00±0.60	13.44±0.27
IM17-81	5.49±0.12a (100)	1.98±0.11b (77)	41.62±2.13ac (110)	6.70±0.42	11.79±0.26

487

488

489

490 **Table 2** Variation between the RNAi transgenic line and WT plants with respect to the expression of grain surface area
 491 (GA), perimeter (GP), length (GL) and width (GW). Values followed by different letters differ significantly ($P \leq 0.01$)
 492 from one another. To facilitate comparisons, all values are also reported (in parentheses) in the form of a percentage of
 493 the corresponding WT value

Lines	Area (GA) (mm ²)	Perimeter (GP) (mm)	Length (GL) (mm)	Width (GW) (mm)
Svevo	18.13±0.17a (100)	18.90±0.11a (100)	7.78±0.04a (100)	3.10±0.02a (100)
IM17-15a	19.64±0.20b (108)	19.39±0.11b (102)	7.93±0.05a (102)	3.25±0.02b (105)
IM17-33aII	20.57±0.16c (113)	20.19±0.09c (107)	8.30±0.038b (107)	3.26±0.02b (105)
IM17-81	18.95±0.19b (104)	19.10±0.11ab (101)	7.79±0.039a (100)	3.19±0.02b (103)

494

495 **Supplementary materials**496 **Table S1.** PCR primer sequences

497

498 **Table S2.** Segregation data in the T₁ generation of the GW2-RNAi transgenic lines

499

500 **Table S3.** Proteins identified by LC-MS/MS analysis in the mature grains of Svevo and IM17-33aII

501

502 **Table S4.** Proteins considered to be unequivocally identified are highlighted in bold

503

504 **Table S5.** [no caption]

505

506

507 **Fig. S1.** The pRDPT-GW2(RNAi) construct

508

509 **Fig. S2.** Alignment of *GW2* cDNAs. The full length coding region (1,275 nt) of the two homeologs (*GW2-A1* and *-B1*)
510 are 98.35% identical

511

512 **Fig. S3.** Alignment of the *GW2* polypeptide encoded by durum wheat cv. Svevo. The NES motif and RING domain are
513 highlighted in, respectively, green and grey. The cysteine and histidine residues belonging to the RING domain which
514 are involved the formation of a zinc finger are numbered and shown in red

515

516 **Fig. S4.** Polypeptide alignment of *GW2* proteins encoded by a selection of grass species. Conserved residues are
517 highlighted in grey, the RING domain in red, the NES motif in green; the Q/R substitution in the RING domain of the
518 rice protein is shown in yellow. TaGW2, TaGW2-A1, TaGW2-B1: from bread wheat, OsGW2: from rice, BdGW2: from
519 *B. distachyon*, HvGW2: from barley, ZmGW2: from maize; SbGW2: from sorghum; SiGW2: from foxtail millet

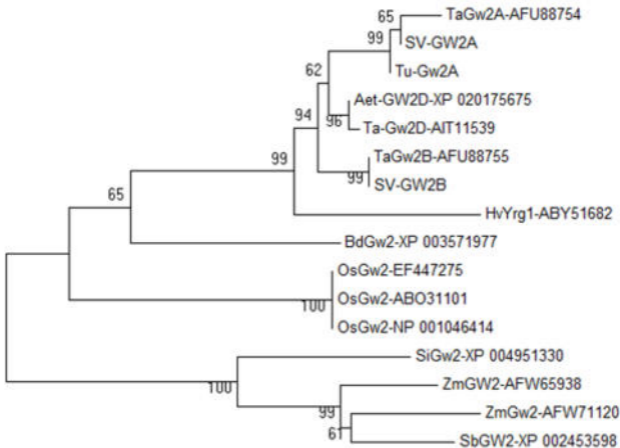
520

521 **Fig. S5.** Fold changes in a) the protein absent from the IM17-33aII proteome but present in the WT proteome, b) the
522 proteins up-regulated in IM17-33aII

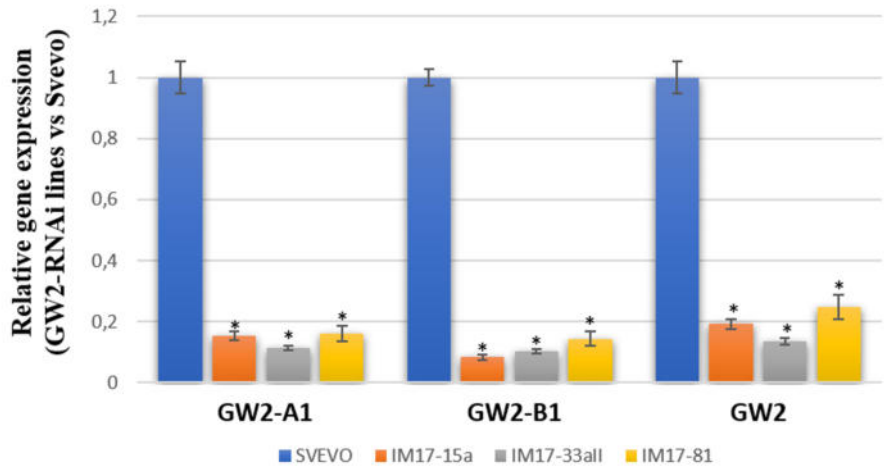
523

524 **Fig. S6.** Alignment of identified proteins

525



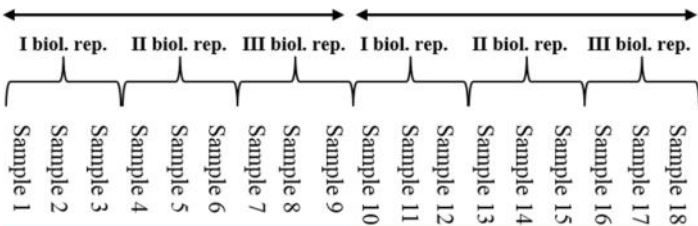
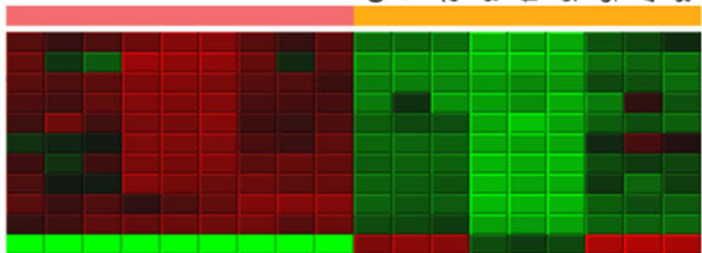
0.020





IM17-33aII

Svevo

11
10
9
8
7
6
5
4
3
2
1Log₂(ratio)

IM17-33aII
Svevo

